Cyclization and Self-Organization in Polymerization of Trialkoxysilanes

Libor Matějka,* Oxana Dukh, Drahomíra Hlavatá, Bohumil Meissner, and Jiří Brus

Institute of Macromolecular Chemistry, Academy of Sciences of the Czech Republic, Heyrovský Sq. 2, 162 06 Prague 6, Czech Republic

Received January 23, 2001; Revised Manuscript Received June 25, 2001

ABSTRACT: Sol−gel polymerization of organotrialkoxysilanes $RSi(OR')_3$ and formation of silsesquioxane (SSQO) structures was followed using SEC, ^{29}Si NMR, and both small- and wide-angle X-ray scattering. Evolution of the SSQO structure is controlled by the competition between intermolecular polycondensation and cyclization. A strong tendency to buildup of polyhedral cyclic oligomers—mainly octamer "cages" and larger cagelike structures—was found to grow with increasing size of substituent R. As a result, long substituents prevent gelation of the trifunctional system and increase stability of the SSQO. Because of incompatibility of the polyhedral SSQO framework and pendant organic chains, microphase separation takes place and spontaneous self-organization occurs. A micellar arrangement of compact SSQO domains with a correlation distance corresponding to the size of the substituent is formed, and the ordering is promoted by increasing length of the organic chain. The most organized arrangement was observed with the trialkoxysilanes substituted with long PEO chains which crystallize and force the SSQO cages to align in the lamellar structure.

Introduction

Trialkoxysilanes $RSi(OR')_3$ with an organic substituent R are suitable precursors of organic−inorganic (O−I) hybrid materials. They also serve as efficient coupling agents increasing compatibility between organic and silica phases. The sol−gel polymerization of trialkoxysilanes involving hydrolysis and condensation results in formation of polysilsesquioxane (polySSQO) $(RSiO_{3/2})_n$ products generally denoted T_n. It is well-known that in addition to an intermolecular polycondensation, alkoxysilanes undergo pronounced cyclization.[1,2] The SSQOs are composed of random branched polymers, ladder polymers and also compact cyclic polyhedral products—"cages".[2−4] Mainly the cages [4−6] formed by the intramolecular condensation are the subject of intense research because of a well-defined compact molecular structure. Recently Eisenberg et al.[7] and Wallace et al.[8] proved cyclization and cagelike clusters in the polymerization of trialkoxysilanes using MALDI−TOF MS. Loy,[9,10] Fasce et al.,[11] and Wallace[8] et al. have shown a significant influence of substituent R on the SSQO structure, steric and charge effects or H-bonding being crucial for the polymerization. The polyhedral SSQO with organic functionalities can be employed as functional molecular building blocks for synthesis of O−I polymers and networks with defined architecture.[12−14] Such nanocomposites with nanosized silica/SSQO domains show interesting mechanical and thermal properties. Research is also focused on layered O−I nanocomposites prepared using surfactants and template polymerization. The template mechanism was initially employed for synthesis of mesoporous silica materials[15] applying a supramolecular self-assembly of organic molecules in a surfactant-silica medium. Ukrainczyk et al.[16] used trialkoxysilanes to prepare layered O−I nanocomposites, Al− and Mg−SSQOs in the absence of a surfactant. The buildup of a well-organized layered structure was achieved by template polymerization of hydrolyzed trialkoxysilanes self-assembled into lamellar micelles. Also others[17] have placed polySSQOs in surfactant templated arrays.

The sol−gel polymerization of (3-glycidyloxypropyl)-trimethoxysilan (GTMS), studied in our previous paper,[18] leads to formation of the functional cage. A stable oligomer fraction was isolated and identified by electrospray ionization mass spectrometry (ESI−MS) and ^{29}Si NMR as a cubic octamer, T_8, with pendant epoxy groups. It was found that the extent of this polyhedral oligomer increases with water content in hydrolysis and dilution of the reaction mixture. In the present paper, the polymerization of various organotrialkoxysilanes was followed, and the effect of the substituent size on the SSQO structure evolution, extent of cyclization—the cage formation—and gelation have been investigated. Very long chains as substituents up to $M = 5000$ were included in the research. So far only two systematic studies of the organic group R influence on gelation of trialkoxysilanes were performed,[9,10,19] using, however, considerably smaller substituents. Attention was also paid to the spatial arrangement and possible self-organization in the sol−gel polymerization at absence of a surfactant. The goal of the research was to study the relations between the reaction mechanism, self-assembly of the system, tendency to cyclization and buildup of polyhedral frameworks and/or gelation as functions of the substituent in the trialkoxysilane and catalytic conditions of the sol−gel process. In addition, the investigation made possible to find out conditions for enhancing stability of functional SSQO intended for synthesis of nanostructured well-defined O−I hybrids. The polymerization and structure evolution were characterized by small- and wide-angle X-ray scattering (SAXS, WAXS), size exclusion chromatography (SEC), and ^{29}Si NMR spectroscopy.

Experimental Section

Materials. The following organotrialkoxysilanes $RSi(OR')_3$, both with and without a reactive functionality in the organic substituent R, were used as obtained from ABCR GmbH & Co.KG: (3-glycidyloxypropyl)trimethoxysilane (GTMS), methyltrimethoxysilane (MTMS), vinyltriethoxysilane (VTES), triethoxysilane (TRES), octyltriethoxysilane (OTES), and (3-isocyanatopropyl)triethoxysilane (ITES). In addition, the

10.1021/ma010136x CCC: $20.00
Published on Web 08/29/2001

trialkoxysilanes with a long nonfunctional chain R were prepared by a modification of oligomeric alcohols or amines. The silane-modified oligomers based on poly(ethylene oxide), SPEO, or poly(propylene oxide), SM, were synthesized by the reaction of poly(ethylene glycol) monomethyl ether (PEO350, PEO750, PEO2000, PEO5000) or poly(propylene oxide)monoamine (Jeffamine, M600 and M2000) of various molecular weights, (M = 350−5000) with a stoichiometric amount of ITES (eqs 1 and 2). The reaction catalyzed with dibutyltin dilaurate (DBTDL) proceeded 1 day at 80 °C, and completeness of the conversion was checked by IR spectroscopy from disappearance of the NCO peak at 2272 cm^{-1}.

$$\underset{\text{PEO}}{\text{R}-\text{OH}} + \underset{\text{ITES}}{\text{OCN}(\text{CH}_2)_3\text{Si}(\text{OCH}_2\text{CH}_3)_3} \rightarrow \underset{\text{SPEO}}{\text{R}-\text{OCONH}(\text{CH}_2)_3\text{Si}(\text{OCH}_2\text{CH}_3)_3} \quad (1)$$

$$\underset{\text{M}}{\text{R}^1-\text{NH}_2} + \text{OCN}(\text{CH}_2)_3\text{Si}(\text{OCH}_2\text{CH}_3)_3 \rightarrow \underset{\text{SM}}{\text{R}^1-\text{NHCONH}(\text{CH}_2)_3\text{Si}(\text{OCH}_2\text{CH}_3)_3} \quad (2)$$

$$\text{R} = \text{CH}_3\text{O}(\text{CH}_2\text{CH}_2\text{O})_n\text{CH}_2\text{CH}_2$$

$$\text{R}^1 = \text{CH}_3(\underset{\text{CH}_3}{\text{CH}_2\text{CHO}})_n \underset{\text{CH}_3}{\text{CHCH}_2}$$

Polymerization Procedure. The sol−gel polymerization of the trialkoxysilanes was performed in bulk or in solution (isopropyl alcohol, THF or dioxane) in the presence of a stoichiometric amount of water, H_2O:Si = 1.5, at temperatures T = 20, 80, or 135 °C. Three types of catalysts were used: acidic, *p*-toluenesulfonic acid (TSA); basic, benzyl (dimethyl)-amine (BDMA); and neutral, DBTDL. A variety of products was obtained, from low-viscosity liquids up to hard gels, with both transparent or slightly opaque appearances.

Methods. Evolution of the structure during polymerization was followed by time-resolved SAXS experiments using an upgraded Kratky camera. Cu Kα radiation (wavelength λ = 1.54 Å) was employed and registered using a position-sensitive detector [20] (Joint Institute for Nuclear Research, Dubna, Russia). The intensities were taken in the range of the scattering vector $q = (2\pi/\lambda) \sin 2\theta$ from 0.005 to 1.0 $Å^{-1}$ (2θ is the scattering angle). The measured intensities were corrected for sample thickness and transmission, the primary beam flux, and the sample−detector distance. No corrections for the primary beam profile were used.

Crystallization of polySSQOs was determined by wide-angle X-ray scattering (WAXS). The diffractograms of the samples were taken on an automatic powder diffractometer HZG/4A. The Cu Kα radiation was monochromatized with a Ni filter and an amplitude analyzer, and recorded with a scintillation counter. The diffractograms were recorded in the range of the diffraction angle 2θ = 4−40°.

Molecular weight growth during polymerization and final products were characterized by SEC with mixed E and D columns (Polymer Laboratories), THF as a mobile phase, and RI detection. Polystyrene standards were employed for molecular weight calibration and a relatively close agreement with the molecular weights determined by ESI−MS for isolated fractions was achieved. A good description of the molecular weight distribution of polySSQOs using polystyrene standards in the range M = 100−4500 was confirmed by Eisenberg.[7] Preparative SEC was used to isolate the oligomer fraction (column PLgel 10 μm 500 Å, 300 × 25 mm; Polymer Laboratories).

^{29}Si NMR spectra were measured using a Bruker DSX 200 NMR spectrometer at frequencies 39.75 and 200.15 MHz (for ^{29}Si and ^{1}H, respectively). Liquid and/or gellike samples were placed in a 4 mm ZrO_2 rotor with KelF spacer. The number of data points was 6 K, magic angle spinning (MAS) frequency 4 kHz, strength of B_1 field (^{1}H and ^{29}Si) 62.5 kHz. The number of scans for accumulation of ^{29}Si MAS NMR spectra was ca. 5000 to achieve an acceptable signal-to-noise ratio. A repetition delay of 40 s was used. The ^{29}Si scale was calibrated by external standard M_8Q_8 (−109.80 ppm, the highest field signal). The conversion α in the sol−gel polymerization of trialkoxysilanes was determined as $\alpha = (\sum iT^i)/3$, where T^i indicates the fraction of the unit T^i with i siloxane bonds −O−Si− attached to the central silicon. The assignment of the NMR bands of T^i units is as follows:[4,21,22] T^0 from −41 to −43 ppm, T^1 from −48 to −52 ppm, T^2 from −54 to −61 ppm, and T^3 from −64 to −69 ppm. The influence of the ring strain on the chemical shift[22] is also taken into account, e.g., the strain in small three-membered rings brings about a downfield shift. In the case of TRES and VTES, the signals are upfield-shifted; T^3(TRES) = −86 ppm; T^3(VTES) ranges from −80 to −82 ppm.

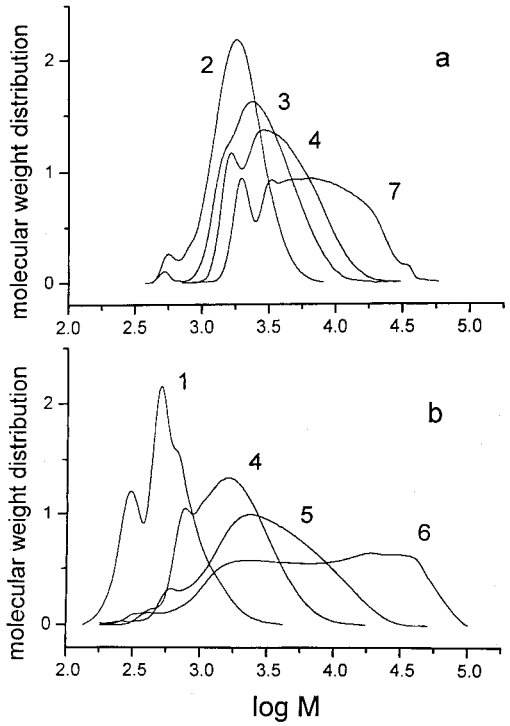

Figure 1. Distribution of molecular weight during polymerization of GTMS catalyzed with (a) DBTDL and (b) TSA. T = 80 °C. Curves: 1, reaction time t = 0; 2, t = 15 min; 3, t = 5 h; 4, t = 24 h; 5, t = 96 h; 6, t = 192 h; 7, t = 360 h.

Results and Discussion

Polymerization of (3-Glycidyloxypropyl)trimethoxysilane (GTMS). Random polymerization of trifunctional monomers like trialkoxysilanes would result in gelation at a conversion α = 0.5, according to the relation:[23] $\alpha_C = 1/(f - 1)$, where α_C is the critical conversion at the gel point and f is the functionality of the monomer. Because of intramolecular reactions, the gel point is shifted to a higher conversion, and with a strong cyclization, no gelation occurs at all.[24−26] This is the case of the GTMS polymerization when polyhedral cyclics are formed under particular reaction conditions.[18] Content of cagelike structures built in the polymerization depends on the catalyst of the sol−gel process. Cyclization is preferred under catalysis with the base BDMA or neutral DBTDL compared to the acid catalysis with TSA. Differences in the reaction course are clear from Figure 1. Fast formation of a stable oligomer fraction is observed using the DBTDL catalyst; however, growth of a high-molecular-weight polymer is suppressed and the system does not gel even at a high conversion α = 0.9 (Figure 1a). The narrow oligomer fraction of the molecular weight $M \sim 1500$ appearing

at the early stage of the reaction involves 15−30% of the reaction product and corresponds to the epoxy functionalized octamer cage as determined by ESI−MS[18] (M = 1336). The amount of this octahedron increases with reaction temperature raising from 20 to 80 °C. ^{29}Si NMR analysis of the corresponding isolated fraction shows almost exclusively branched T^3 silicons belonging to intramolecularly branched polyhedral framework: $T^3 = 0.95$; $T^2 = 0.05$. In the reaction mixture, polyhedral octamer, nonamer, and decamer were determined by ESI−MS. Also higher-molecular-weight polySSQO contains a large amount of cagelike frameworks. The presence of the dimer−cage is indicated by another small peak of a corresponding molecular weight in Figure 1a (curve 7). NMR data of the reaction mixture polymerized to a high conversion reveal no terminal T^1 silicons and a high fraction of branched T^3 units: $T^1 = 0$; $T^2 = 0.31$; $T^3 = 0.69$. While terminal T^1 silicon is characteristic of noncyclic structures, one can consider three types of T^3: (a) intermolecular branching point, (b) unit belonging to a cycle within a linear chain with two intermolecular branches, and (c) intramolecular branching unit in the polyhedron issuing no chain from the molecule, which prevails in this case. On the contrary, a very small amount of cages is formed in the GTMS polymerization under acid catalysis with TSA. No stable oligomer fraction could be detected in the polymerization (Figure 1b). The intermolecular condensation is preferred; a high-molecular-weight branched polySSQO grows, and the system finally gels at a conversion $\alpha = 0.72$. Composition in the gel state exhibits a considerably higher amount of T^1 silicones, a larger fraction of linear sequences T^2, and a smaller fraction of T^3 compared to the previous system: $T^1 = 0.12$; $T^2 = 0.60$; $T^3 = 0.28$. Under the acid catalysis, however, T^3 silicons are involved mainly in the intermolecularly branched units representing cross-links in the polymer network. In addition to the sol−gel reactions of the alkoxy groups one has to take into account also the reaction of the epoxy group present in GTMS. Hydrolysis of the epoxy ring and the subsequent condensation of forming C−OH with Si−OH were detected[18] using ^{13}C NMR. However, the reaction of the epoxy group is much slower compared to the alkoxy ones and does not affect the structure growth at initial and medium polymerization stages.[18] Only at a very late stage does the reaction of the epoxy groups become more important, and it may impact a polymer growth and initiate or accelerate gelation of the system.

Figure 2 shows the structure evolution in polymerization of GTMS followed by SAXS. The reaction mixture was concentrated before the measurement by removing methyl alcohol evolved in the sol−gel reaction. We suppose that the maximum of intensity on the SAXS profile of the initial reaction mixture at $q \sim 0.6$ Å^{-1} (curve 1), characterizes intramolecular distances in GTMS and products. A similar high-q maximum is observed also with other trialkoxysilanes. During the polymerization catalyzed with DBTDL, a new maximum at $q \sim 0.4$ Å^{-1} appears and gradually grows in Figure 2a. In addition, a slight broader second maximum is detected at $q \sim 0.15$ Å^{-1}. Similar development of the SAXS profiles was found in the polymerization under catalysis with BDMA. The maximum at $q \sim 0.4$ Å^{-1} becomes apparent only at a high conversion, $\alpha > 0.7$, due to its overlap with the high-q peak at $q \sim 0.6$ Å^{-1}. At this conversion intramolecularly branched T^3 units

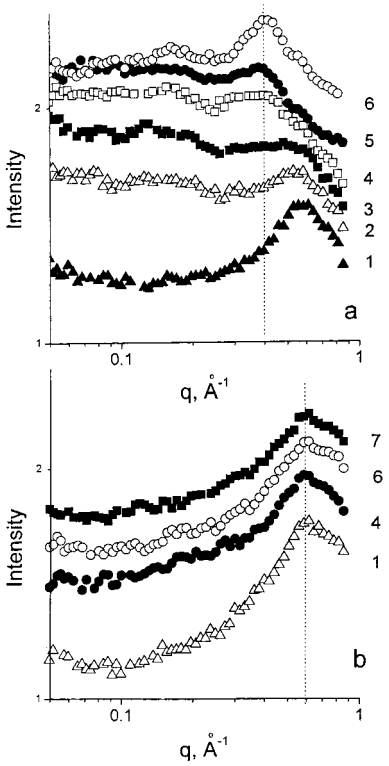

Figure 2. Development of SAXS intensity profiles during sol−gel polymerization of GTMS catalyzed with (a) DBTDL or (b) TSA. T = 20 °C. Curves: 1, reaction time t = 5 min; 2, t = 90 min; 3, t = 3 h; 4, t = 8 h; 5, t = 48 h; 6, t = 168 h; 7, t = 336 h. Curves 1−7 are mutually vertically shifted.

become predominant in the polySSQO structure, $T^3 > 0.4$, and the system is filled up with cagelike structures**.** Both maxima at $q = 0.40$ and 0.15 Å^{-1} are assumed to be interference maxima coming from scattering on regularly arranged heterogeneities − compact frameworks separated by an organic substituent. To prove this, we dissolved the reaction mixture in isopropyl alcohol and applied the SAXS measurements on the dilute system. The SAXS curves then changed dramatically as can be seen in Figure 3. While the high-q maximum (0.6 Å^{-1}), originating from intramolecular distances, was still observed, both peaks at $q \sim 0.15$ Å^{-1} and $q \sim 0.40$ Å^{-1} disappeared (Figure 3a), which is an evidence of intermolecular interference. For sufficiently dilute mixtures, the SAXS curve provides a scattering characteristics of an individual cluster. The slope (x) of the intensity log−log profile (intensity vs q) of dilute systems in the Porod region is quite steep in the case of DBTDL catalysis, x(DBTDL) ~ 3 (Figure 3a), revealing a very compact "particle-like" cluster framework. In contrast, a loose structure of linear and branched polySSQOs is formed under acid catalysis, x(TSA) ~ 1.4 (Figure 3b). The position of the intermolecular interference maximum in the bulk system corresponds to the correlation distance between the heterogeneity domains—cages—separated by pendant organic substituent R-3-(glycidyloxy)propyl group. A theoretical estimate of the separation distance is $d_1 \sim 15$ Å (length of the R group, 9.5 Å, and the cage diameter, 5.5 Å) corresponding to $q_{1\max} (=2\pi/d_1) = 0.42$ Å^{-1}, which is in agreement with experiment. SAXS measurement of the reaction mixture without removal of volatiles shows a less pronounced maximum. The main interference maximum appears only at a higher conversion and, moreover, at a lower q value; $q_{\max} = 0.32$ Å^{-1}. This is possibly a consequence

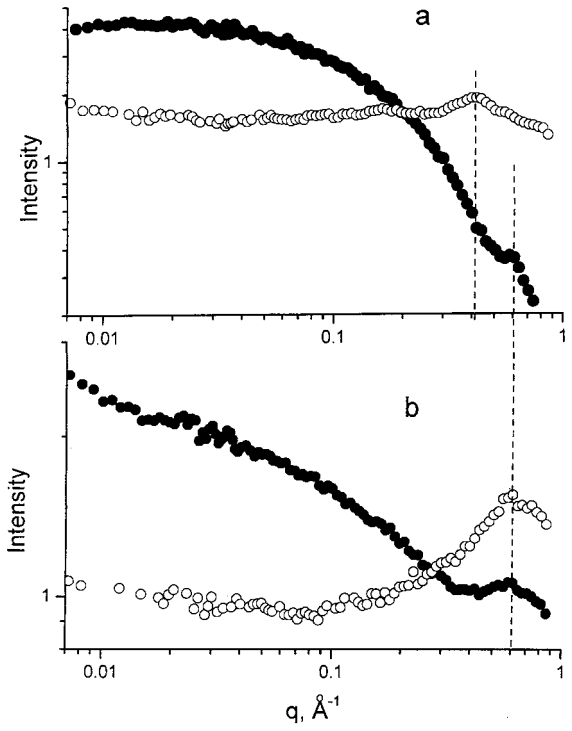

Figure 3. SAXS curves of the polymerized GTMS formed under catalysis with (a) DBTDL or (b) TSA: (○) reaction mixture: (●) after dissolution in isopropyl alcohol.

of swelling of the organoSSQO in the methyl alcohol−water medium leading to an increase in correlation distance.

The results can be interpreted as follows: hydrolysis and condensation of GTMS leads to a spontaneous self-organization without any surfactant present. The structure is organized into micelles with the compact SSQO polyhedral core and protruding glycidyloxypropyl groups. The length of the organic group of these octopus-like molecules determines the separation distance of the cages as shown in Scheme 1a. In addition to the octamer the broad molecular weight distribution of polyhedral SSQO appears, including dimer−cage, etc. In our previous ESI−MS analysis,[18] the incompletely condensed cages were also determined in the reaction system, and those appearing in the highest amount are shown in Scheme 2. These functional SSQO frameworks (octa-, nona-, and decahedrons) can interconnect and serve as building units for a higher molecular weight polyhedral SSQO. Mono-, bi-, tri-, and tetrafunctional molecular blocks in Scheme 2 can form linear and branched polyhedral structures. An appearance of polyhedral networks is not probable because of a low content of the tri- and tetrafunctional units.[18] Moreover, due to steric hindrance even the tetrafunctional cage would preferably undergo a linear condensation. The possible interconnection is indicated in Scheme 1b. This is in agreement with the finding of Eisenberg et al.[7] that most species are incompletely condensed and the SSQO structure is built by combining fundamental octamer building blocks. On the basis of our results we cannot exclude the ladder structure in a high-molecular-weight polymer. However, the data prove a fast formation of small polyhedrons and their interconnection in a higher molecular weight polyhedral structure is most probable. The increasing size of a polyhedral SSQO cluster as well as the corresponding increase in steric hindrance preventing interpenetration of the organic groups of different clusters result in a larger separation distance. The second broad maximum at $q_{2max}\sim0.15$ Å^{-1} could be assigned to less organized dimeric or larger polyhedral

Scheme 1. Ordering of Cagelike Structures in the Polymerized GTMS[a]

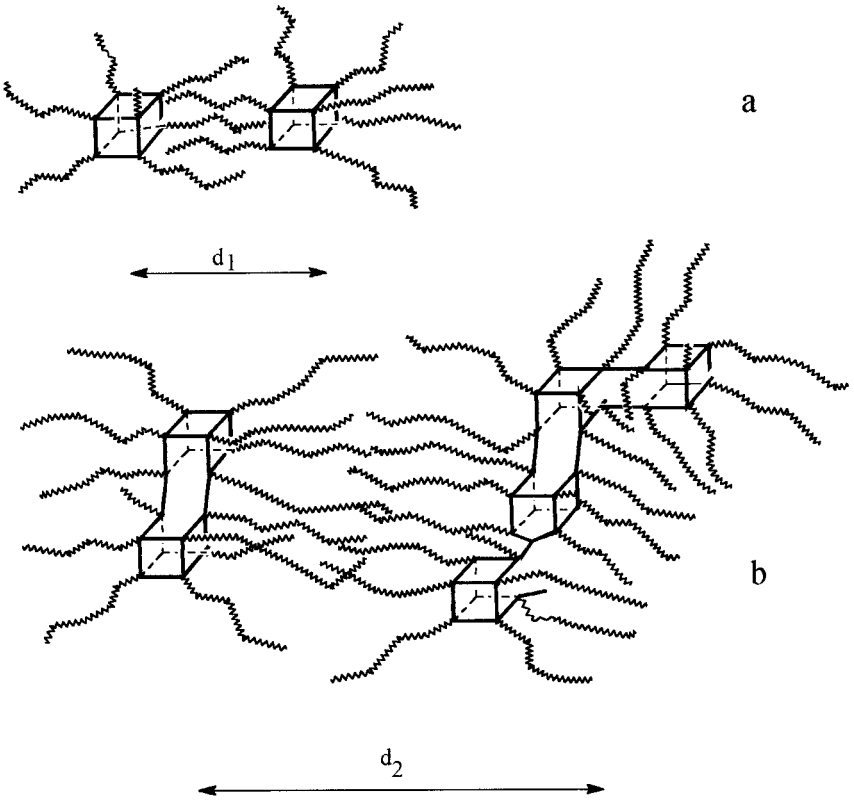

[a] Key: (〰) glycidyloxypropyl group.

Scheme 2. Incompletely Condensed SSQO Cages Determined in Polymerized GTMS,[18] Where the Glycidyloxypropyl Substituent Is Neglected

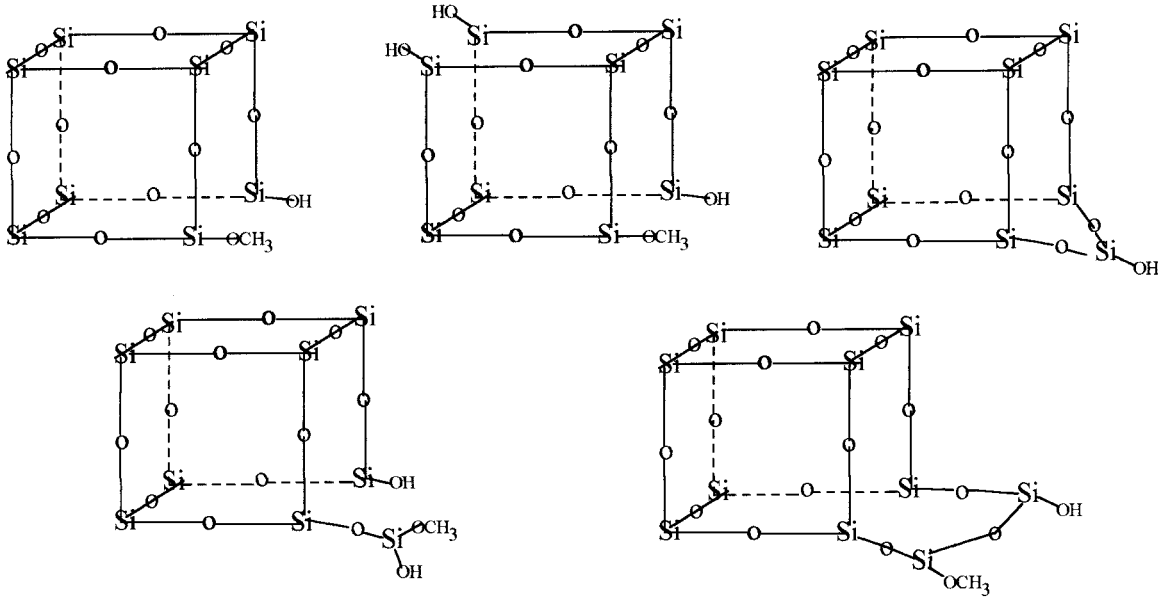

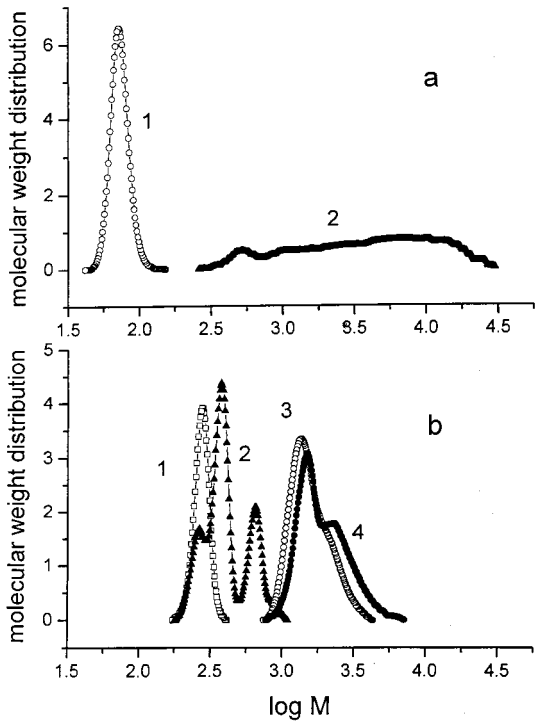

Figure 4. Distribution of molecular weight during polymerization of (a) MTMS and (b) OTES under TSA catalysis: (a) $T = 20$ °C; (b) $T = 80$ °C; isopropyl alcohol solution. Curves: 1, $t = 0$; 2, $t = 15$ min; 3, $t = 96$ h; 4, $t = 47$ days. The ordinate for peak 1 for part b was arbitrarily decreased.

structures. Scheme 1 suggests possible polyhedral SSQO structures and ordering.

No interference maxima at $q < 0.50$ Å^{-1} are observed in polymerization under TSA catalysis in Figure 2b. Only the initial intramolecular interference maximum at $q \sim 0.6$ Å^{-1} can be seen. The microphase separation making a self-assembly of the regularly arranged domains, does not occur in this case. In the acid polymerization, a broad distribution of high-molecular-weight polySSQOs with dangling organic substituents is formed; the structure does not promote any ordering. Moreover, unlike the compact SSQO frameworks filling the system under DBTDL catalysis, loose polymer coils are spread in the acid medium as is apparent from the slope in Figure 3.

Effect of Substituent in the Trialkoxysilane Polymerization. We have polymerized a series of trialkoxysilanes with various lengths of the substituent, including trialkoxysilyl-modified poly(ethylene oxide)s and poly(propylene oxide)s of molecular weights 350−5000, and studied the effect of the substituent size. Figures 4 and 5 show the growth of polySSQO molecular weight during the sol−gel polymerization. The reaction rate substantially decreases with increasing length of the substituent. Polymerization of small trialkoxysilanes, like triethoxysilane (TRES, R=H), methyltrimethoxysilane (MTMS, R = CH_3) (Figure 4a) and vinyltriethoxysilane (VTES, R = CH_2=CH) is relatively fast, and the system gels under both basic and acid catalysis. (In the case of TRES one has to take into account hydrolysis of SiH to form a tetrafunctional monomer leading to the silica network.) The presence of a longer organic group in octyltriethoxysilane (OTES, R=$CH_3(CH_2)_7$) (Figure 4b) and in the silane-end-capped oligomers SPEO and SM (Figure 5) leads to the formation of low-molecular-weight SSQO products only and prevents gelation of the system. The resulting SSQO species are quite stable.

In the polymerization of OTES (in isopropyl alcohol solution) under TSA catalysis, the monomer is quickly depleted (Figure 4b); however, the polycondensation is slow. The fraction of oligomers with the SEC peak centered at about polymerization degree $n = 5$ (curve 3) (using polystyrene calibration) is very slowly transformed to higher molecular weight products after the monomer consumption. At a late reaction stage, the fraction with a small peak centered at the octamer (curve 4) becomes significant. No polymer with $M >$ 5000 appears even at a high conversion, ($\alpha = 0.94$). The ^{29}Si NMR spectrum of the reaction mixture in Figure 6 shows bands in the regions corresponding to T^2 (−54 to −61 ppm) and T^3 (−64 to −68 ppm) silicons. The absence of terminal T^1 units in such low-molecular-weight products proves cyclic structures. Moreover, according to the analysis, the observed T^3 belong

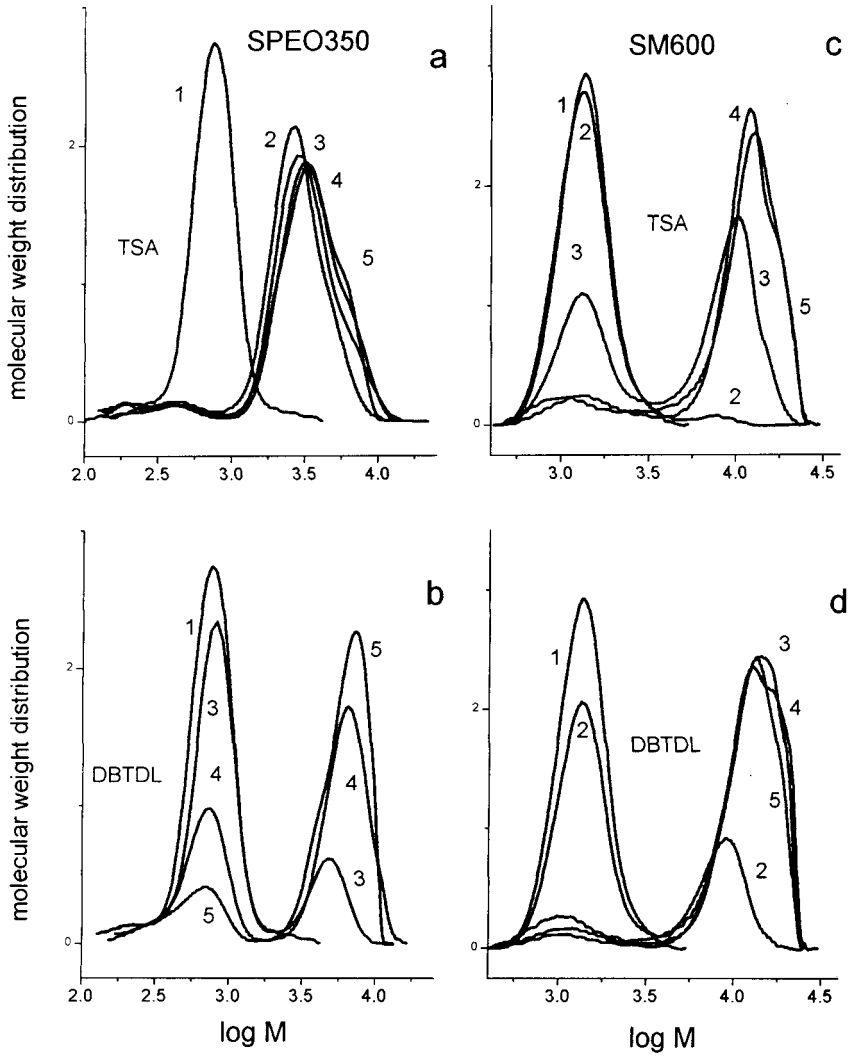

Figure 5. Distribution of molecular weight during polymerization of SPEO350 and SM600 at 80 °C under TSA or DBTDL catalysis: (a) SPEO350/TSA; (b) SPEO350/DBTDL; (c) SM600/TSA; (d) SM600/DBTDL. Curves: 1, $t = 0$; 2, $t = 1$ h; 3, $t = 24$ h; 4, $t = 120$ h; 5, $t = 288$ h.

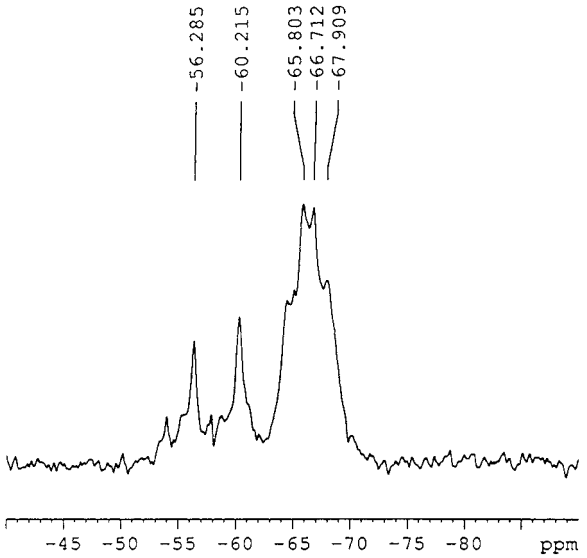

Figure 6. ^{29}Si NMR spectrum of the polymerized OTES formed under TSA catalysis in isopropyl alcohol solution. $T = 80$ °C; $t = 10$ days.

exclusively to the intramolecularly branched silicon units because, at the nonoccurrence of T^0 and T^1, any amount of intermolecular branching would lead to gelation. Hence, the results give an evidence of polyhedral cyclic frameworks in oligomeric octyl-substituted SSQOs. The band at −66.7 ppm is attributed to T^3 silicon in octahedron T_8 [22,27] and the next band at −67.9 ppm could possibly belong to T^3 units in incompletely condensed cages in trisilanol $T_7(OH)_3$ (i.e., $R_7Si_7O_9(OH)_3$) or disilanol $T_8(OH)_2$ (i.e.,$R_8Si_8O_{11}(OH)_2$).[4] The chemical shift of the less strained octyl-substituted decahedron T_{10} is −68.7 ppm. [22] Perhaps a small amount of T_{10} could be expected to be hidden in the broad asymmetric peak in Figure 6. As high power ^{1}H decoupling and MAS at 5 kHz were used in acquisition of NMR signals, the observed broadening of the signals is inhomogeneous resulting from variation of local magnetic fields around silicon nuclei (^{29}Si chemical shifts are highly sensitive to small changes in local magnetic fields, which results in wide dispersion of chemical shifts). No larger polyhedrons are present because of the absence of bands in the region above −70 ppm.[22] The bands of T^2 silicons in the −57 to −61 ppm region can be interpreted by the existence of different diastereoisomers of an incompletely condensed octahedron $T_8(OH)_2$[4,11,21] while the sharp band at −60.2 ppm could be assigned to trisilanol $T_7(OH)_3$.[4] The intense peak at −56.3 possibly originates from the T^3 silicon of the more strained three-membered ring in hexahedron

T_6.[4] ^{1}H NMR analysis shows that in isopropyl alcohol solution a transesterification of OTES takes place and about 20% of the ethoxy groups are replaced with isopropoxy ones under the reaction conditions used. This fact does not impact the above data interpretation.

Only a small content (~10%) of stable oligomer cyclics was found in the polymerization of the short trialkoxysilane MTMS (Figure 4a). The intermolecular polycondensation is preferred in this case. The high-molecular weight polymer grows, the molecular weight distribution (dW/d(log M)) is very broad, and finally, a network is built.

The effect of the sol−gel catalysis on polymer growth is observed in Figure 5. Polymerization of the silane modified oligomers SPEO350 and SM600 under DBTDL catalysis leads to a bimodal distribution of molecular weights with the gradually consumed "macromonomer" SPEO350 or SM600 and the formed "macrooctamer" (see Figure 5, parts b and d). The peak of the growing oligomer fraction is centered at $n \sim 6.5$ and shifted to $n \sim 10$ (based on polystyrene standards) with increasing reaction time. No small intermediates, dimer or trimer, were detected by SEC revealing the preferable buildup of the stable medium-size oligomer (octamer). Acid catalysis with TSA promotes rapid hydrolysis and faster monomer consumption in Figure 5a compared to the neutral DBTDL catalysis in the case of SPEO 350 (Figure 5b). However, polycondensation is slower using TSA, and gradual growth of the full distribution of small oligomers including dimer and trimer occurs without preferable formation of octamer. Polymerization of SM600 under DBTDL is faster compared to SPEO350 (cf. Figure 5, parts b and d) because of slight internal base-catalysis by the catalytically active urea group present in the SM600 molecule (see eq 2). An effect of the urea was proved by using a model urea catalyst for the sol−gel reaction of SPEO350 that does not involve an urea group. The reaction catalyzed with DBTDL was accelerated in the presence of tetramethylurea. We suppose that pH-neutral DBTDL advances hydrolysis and urea accelerates the subsequent condensation. The effect of acidic catalysis with TSA is neutralized in SM600 and the reaction is slower than when using DBTDL (cf. Figure 5, parts c and d). However, no significant difference in the molecular weight distribution was observed in TSA and DBTDL catalysis (cf. Figure 5, parts c and d). In both cases (SPEO and SM), no high molecular weight polymer grows and the trialkoxysilanes do not gel despite high conversion ($\alpha = 0.94$). The fraction of the oligomer product in polymerization of SM600 corresponding to the polymerization degree $n = 8.7$ was isolated by the preparative chromatography and analyzed by ^{29}Si NMR. The following distribution of T^i units, $T^1 = 0$, $T^2 = 0.18$, and $T^3 = 0.82$, proves the polyhedral cyclic structure of the octamer as discussed above. The relatively high amount of T^2 silicons, characterizing unbranched sequences, can be accounted for by the presence of incompletely condensed cages in the isolated fraction. In the reaction mixture, intermolecular combining of the open cages, e.g. $T_8(OH)_2$, leads to a mild increase in the molecular weight and broadening of the distribution by formation of larger structures, e.g., dimer−cage. At a high conversion ($\alpha = 0.94$) the polySSQO is composed of polyhedral frameworks only as is apparent from the low molecular weight and the distribution of T^i units: $T^1 = 0$, $T^2 = 0.215$, and $T^3 = 0.785$ for SPEO350 and $T^1 = 0$, $T^2 = 0.175$, and $T^3 = 0.825$ for SM600.

The results imply an increasing tendency to cyclization in polymerization of organotrialkoxysilanes with a long substituent. While small trialkoxysilanes like MTMS undergo intermolecular branching and gelation, enhancing steric hindrance due to an organic chain strongly favors an intramolecular reaction and cyclics formation at the expense of the intermolecular condensation. As a result, the polyhedral octamer and larger cagelike frameworks are built. In the case of GTMS, under DBTDL catalysis, the octamer fraction is formed; however, the broad molecular weight distribution of polyhedral SSQO is also observed. With further increasing length of R, the incompletely condensed cages (see Scheme 2) arising at the early stage are prevented from close approach due to the separating R group (cf. Scheme 1) and cannot combine into higher molecular weight polyhedral polymers. The SiOH react intramolecularly yielding a narrow distribution of almost fully condensed frameworks which are very stable (see Figures 4b and 5).In accordance, Feher[28] and Fasce et al.[11] observed a high yield of polyhedral oligoSSQOs in the polymerization of trialkoxysilanes with sterically demanding substituents, the octahedron and decahedron being the main species. In contrast, a broad distribution of incompletely condensed species was found in the polymerization of the trialkoxysilane with the less bulky substituent.[11] High extent of cyclization was also detected by Wallace[8] for long alkyl (decyl) chain as R. However, he did not find a simple trend between the size of the substituent and cyclization and assumed that partial-charge effects and hydrogen bonding must be taken into account. Mainly phase separation, in addition to steric hindrance of the bulky or long alkyl substituents and corresponding limitation of the conversion were reported by Loy[9] to be the reasons for inability of the trialkoxysilanes to gel. In our experiments, OTES was polymerized in the homogeneous isopropyl alcohol solution and no phase separation occurred even in the polymerization of SPEO and SM oligomers because of small amount of water in stoichiometric mixtures (H_2O:Si = 1.5). Moreover, the small propensity to gelation of the trialkoxysilanes with long organic chains is not due to kinetic reasons and lower reactivity of these systems as all studied trialkoxysilanes reached a quite high conversion; $\alpha > 0.9$. Consequently, our results prove that the pronounced cyclization and buildup of polyhedral frameworks is the main reason for suppression of gelation in trialkoxysilanes with long substituents. In accordance, the theoretical treatment of Rankin et al.[29] shows that preferred formation of polyhedral cyclics is crucial for shift of gelation in the sol−gel polymerization of alkoxysilanes. The results also implies an important effect of the long R group on the stability of the SSQO due to steric restrictions of the intermolecular condensation and a high fraction of fully condensed species.

Self-Organization during the Sol−Gel Process. The SSQO structure evolution in polymerization of organotrialkoxysilanes is determined by a competition between the intermolecular polycondensation and intramolecular reactions to form cyclics and cages. Moreover, we have found that it is controlled by a spontaneous self-organization taking place during the reaction. Long substituents in trialkoxysilanes promote the polyhedral framework formation and also ordering of the reaction system. The structure evolution in polymerization of the trialkoxysilane with a long organic chain,

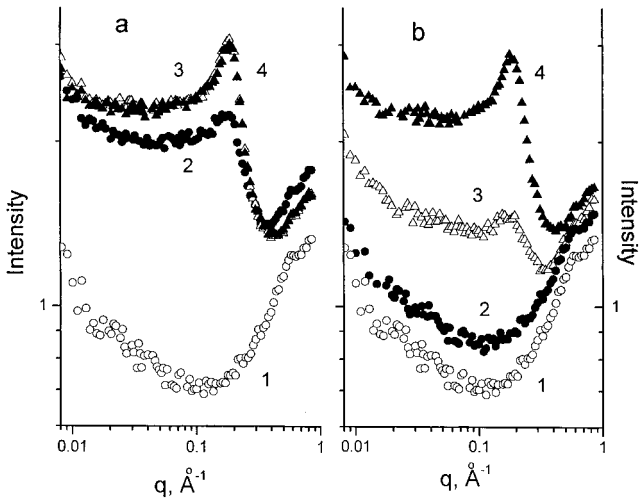

Figure 7. Evolution of SAXS profiles during polymerization of SM600 under (a) DBTDL and (b) TSA catalysis. $T = 80$ °C. Curves: 1, $t = 0$; 2, $t = 5$ h; 3, $t = 24$ h; 4, $t = 120$ h.

SM600, followed by SAXS is given in Figure 7. The sharp maximum growing at $q = 0.18$ Å^{-1} reveals a microphase separation and a high degree of ordering of the polyhedral domains. The intensity and sharpness of the maximum increase with the reaction conversion and the cage content. Self-organization occurs both under DBTDL and TSA catalysis unlike the GTMS polymerization. In addition, the maximum is more distinct in this case and appears even without removal of volatiles from the reaction mixture. Faster organization is observed using DBTDL, in agreement with SEC data in Figure 5.

The effect of the trialkoxysilane substituent size and the catalyst type on the SSQO structure arrangement is shown in SAXS graphs in Figure 8. Two maxima at $q = 0.36$ and 0.17 Å^{-1} were observed in the polymerization of OTES (in isopropyl alcohol solution), and pronounced interference maxima characterize the polymerization products of all the studied SPEO and SM oligomers. The position of the maximum correlates with the molecular weight of the organic chain (see Figure 8a), proving that its length controls space separation of the cage frameworks. The q_{max} is shifted to lower values in the polymerized trialkoxysilanes with longer R (cf. $q_{max} = 2\pi/d$). On the contrary, the intensity curves of the polymerized small trialkoxysilanes, TRES and VTES, do not show any maximum at $q < 0.50$ Å^{-1}. The intensity increase at low q is given by the large branched and cross-linked SSQO structures. The slight maximum in the case of MTMS corresponds to a low content of polyhedrons as determined by SEC. Figure 8b shows an influence of the catalyst on the ordering of SSQOs with a long substituent. The interference maximum observed in the polymerization of SPEO350 using TSA catalysis is shifted to a higher q value compared to DBTDL catalysis indicating a shorter correlation length. We suppose that a large amount of silanol groups is present in the SSQO framework due to fast hydrolysis under the acid catalysis. As a result an H-bond interaction between SiOH and OCH_2 group of the poly(ethylene oxide) chain occurs and leads to partial interpenetration of the SSQO structures and PEO. Because of this interaction, the separation distance between compact frameworks diminishes. No such difference in q_{max} was observed in the polymerization of SM600, where both TSA and DBTDL catalysis lead

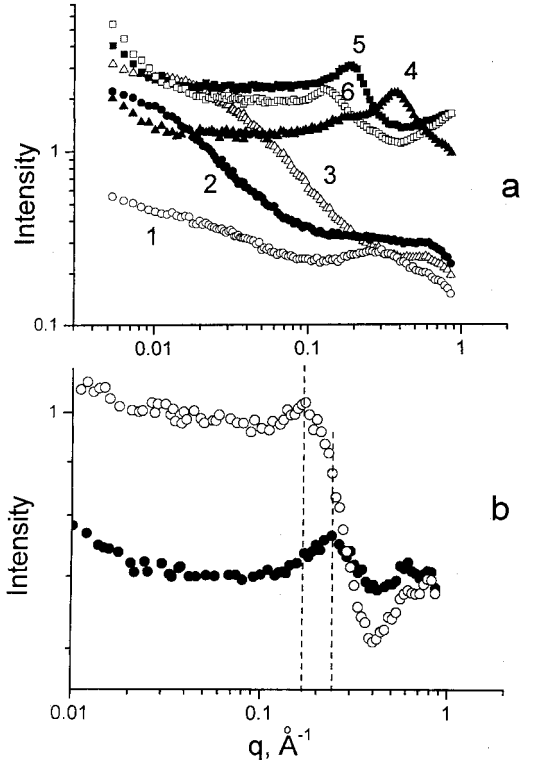

Figure 8. SAXS profiles of the polymerized organotrialkoxysilanes. (a) Curves: 1, MTMS (catalyst DBTDL; reaction time and temperature: $t = 1$ h, $T = 20$ °C); 2, VTES (DBTDL, 1 d, 20 °C, dioxane solution); 3, TRES (DBTDL, 1 d, 20 °C); 4, OTES (DBTDL, 1 d, 80 °C, isopropyl alcohol solution); 5, SM600 (DBTDL, 1 d, 80 °C); 6, SM2000 (DBTDL, 16 d, 20 °C). Curves 4−6 are upward shifted with respect to curves 1−3. (b) SPEO350: (●) TSA catalysis; (○) DBTDL catalysis (7 d, 80 °C).

to self-assembly with $q_{max} = 0.18$ Å^{-1} (cf. Figure 7). This result agrees with the SEC observation that TSA affects the molecular weight distribution in SPEO but not in SM polymerization (cf. Figure 5).

In contrast to the absence of gelation in long trialkoxysilanes discussed above, Shimojima[30] and Loy[10] observed a fast solidification in the polymerization of decyl-, hexadecyl-, and octadecyl(trialkoxy)silanes. In this case, however, no covalent chemical network is built, but it is a thermoreversible physical network due to crystallization of long alkyl chains. We have found a similar effect and a perfect supramolecular ordering in the polymerization of SPEO with a long poly(ethylene oxide) chain of molecular weights $M = 2000$ and 5000. SPEO2000 and SPEO5000 do not gel in the reaction at 135 °C and quickly solidify by cooling the melt down to ambient temperature. SAXS curves of the samples after cooling given in Figure 9 show two maxima at $q = 0.035$ and 0.070 Å^{-1} for the polymerized SPEO2000 and $q = 0.027$ and 0.054 Å^{-1} for SPEO5000. As the main part of SPEO is the poly(ethylene oxide) chain, having a strong tendency to crystallize, we assumed that these peaks are the first and second order of the interference maximum corresponding to the long period L_p of the regular alternation of crystalline and amorphous regions. $L_p = 180$ Å for polymerized SPEO2000, and $L_p = 233$ Å for SPEO5000. The presence of the second-order maximum is indicative of a lamellar structure. Figure 9a shows a comparison of the SAXS profiles of the polymerized SPEO2000 (SSQO) with neat PEO2000 and nonpolymerized SPEO2000. The crystalline structure of PEO2000 exhibits the first-order maximum at $q =$

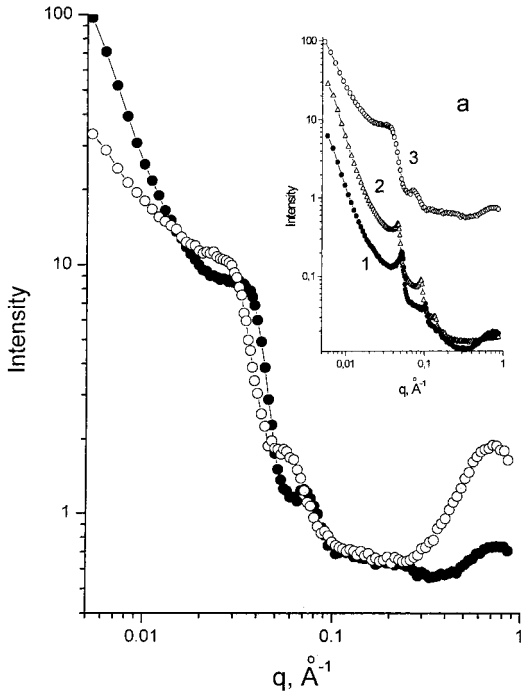

Figure 9. SAXS profiles of SSQOs formed from trialkoxysilanes with long poly(ethylene oxide) substituents: (●) SPEO2000; (○) SPEO5000. (a) Inset: 1, PEO2000; 2, SPEO2000; 3, polymerized SPEO2000.

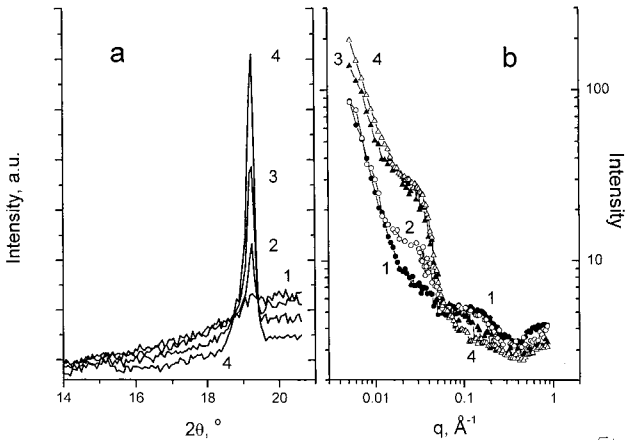

Figure 10. Development of crystallinity at cooling SSQOs formed from trialkoxysilanes with long poly(ethylene oxide) substituent SPEO2000 followed by WAXS (using Kratky goniometer with an elevated camera) (a) and SAXS (b). Curves: 1, t = 11 min; 2, t = 12 min; 3, t = 13 min; 4, t = 14 min. t = time of slow cooling the melt from T = 135 °C.

0.51 Å^{-1} corresponding to the long period L_p = 123 Å. In SPEO2000, the lamellar structure is preserved but with a larger long period, L_p = 150 Å (the maximum is shifted to lower q) due to the larger chain length as apparent from the synthesis in eq 1. After polymerization, a further increase in the long period occurs (L_p = 180 Å). An evidence of crystallization of these SSQOs was obtained by using wide-angle X-ray scattering (WAXS). Development of the crystalline reflection on the WAXS diffractograms of the slowly cooled melt is shown in Figure 10a. The position of this reflection (2 θ = 19.2°) characterizing the crystalline lattice and interchain distance is independent of molecular weight of SPEO and is very close to that found in the crystalline phase of poly(ethylene oxide). Simultaneous with the increasing intensity of the crystalline reflection in WAXS during cooling, development of SAXS profiles was also observed in Figure 10b. The melts of both polymerized SPEO oligomers exhibit SAXS interference maxima: q_{max}(SPEO2000) = 0.16 Å^{-1} (see Figure 10b, curve 1) and q_{max}(SPEO5000) = 0.10 Å^{-1}, corresponding to correlation lengths 39 and 63 Å, respectively, given by the PEO chain length. The theoretical end-to-end distance r for SPEO2000 and SPEO5000 is 40 and 63 Å, respectively, in good agreement with experiment. The expression $r^2 = C_n n l^2$ valid for a sufficiently long flexible chain[31] was applied for calculation (C_n = 4.0 is the characteristic ratio for PEO chain,[31] n is number of bonds, l is bond length). These maxima gradually disappear while cooling, and new maxima given by the supermolecular ordering of crystalline and amorphous regions grow in the low-q region. As is known, the crystalline PEO2000 makes only extended chain lamel-

Scheme 3. Ordering in the Melt and Crystalline Form of Polymerized SPEO

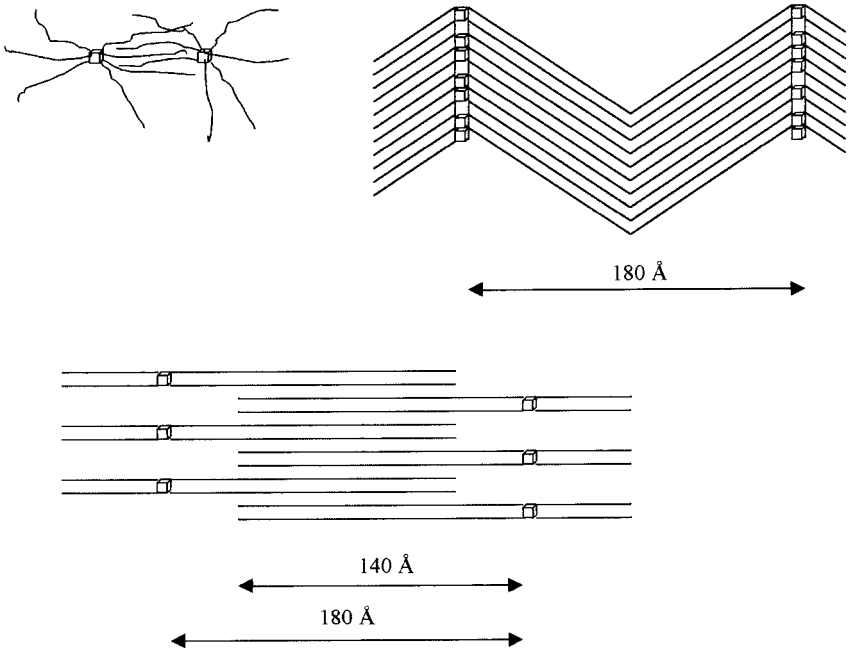

lae[32] with the long period $L_p = 123$ Å. To account for the experimental data of the SSQOs ($L_p = 180$ Å), we propose two possible models of the crystalline structure in Scheme 3: (a) a distorted bilayer lamellar structure or, more probably, (b) a partially interpenetrated structure**.** Other arrangements, however, cannot be ruled out. The Scheme shows also the initial ordering in the melt. In the case of SPEO5000, folded chain lamellae of PEO may appear.[32] The long periods determined for PEO5000 and for neat and polymerized SPEO5000 are $L_p = 153$, 185, and 233 Å, respectively, which is also in agreement with the arrangement in Scheme 3.

The sol−gel process of the SPEO and evolution of the supermolecular structure can be interpreted as follows. During polymerization, self-organization into micellar SSQO domains occurs with a correlation distance corresponding to the PEO coil size in the melt as the PEO chains of different micelles are intertwined (Scheme 3). While cooling, crystallization of fully extended PEO chains in SPEO2000 or folded chains in SPEO5000 take place. This crystallization acts as a driving force for ordering of the SSQO cages into lamellae and the lamellar structure is created.

Conclusions

The structure evolution in the sol−gel polymerization of organotrialkoxysilanes $RSi(OR')_3$ is dependent on the type of the substituent R. Increasing the size of R results in slowing down the polymerization, the intermolecular reaction is sterically hindered, and the cyclization is advanced. Because of cyclization competing with the intermolecular condensation, the trialkoxysilanes with long substituents do not form high-molecular-weight polymers and do not gel even at high conversions. Instead, the narrow distribution of SSQO polyhedrons, with emanating organic chains as octopus-like molecules is formed. The octamer cages proved in isolated fractions as well as larger incompletely condensed polyhedral clusters are the main reaction products. The SSQO with long substituents are stable because of a high fraction of intramolecularly fully condensed species and steric restrictions to intermolecular condensation. The cage buildup is also preferred at high temperatures and in dilute systems. Because of incompatibility of the SSQO framework and pendant organic chains, microphase separation takes place and self-organization into micelles occurs. Evidence of the well-organized structure of regularly arranged domains of compact cagelike frameworks is given by the sharp interference maxima in SAXS intensity profiles. The position of the maximum is determined by the length of organic chains separating SSQO polyhedrons. Long substituents promote the self-organization, the best ordering being achieved for SPEO2000 and SPEO5000 which crystallize in a partially interpenetrated monolayer or a distorted bilayer lamellar structure.

In contradiction, trialkoxysilanes with small substituents undergo faster condensation and intermolecular branching because of lower steric hindrance. As a result, the growth of a high-molecular-weight polySSQO with dangling organic groups is preferred and the system finally gels. A low extent of cyclization and small fraction of polyhedrons were found, no micelles are created, and regular arrangement is absent. Lack of ordering for products of trialkoxysilanes with shorter R was observed also by Ukrainczyk[16] in layered aluminosilsequioxanes.

The catalysis of the sol−gel process determines the reaction mechanism and controls the structure evolution and ordering of the system. While basic and neutral catalysis with DBTDL lead to pronounced cyclization and self-organization, the acid catalyst produces less polyhedral structures and no regular arrangement. The reason is an advanced fast hydrolysis and a high content of −SiOH. An increasing H-bond interaction with oxygen atom in the organic chain leads to a better compatibility, and microphase separation is restricted. By using long substituents, microphase separation occurs even in an acidic medium, but due to partial phase interpenetration, an arrangement with a shorter correlation distance is created.

Acknowledgment. The authors acknowledge financial support of the Grant Agency of the Czech Republic (203/98/0884) and the Grant Agency of Academy of Sciences of the Czech Republic (A4050008).

References and Notes

(1) Brinker, C. J.; Scherer, C. W. In *Sol−Gel Science*; Academic Press: San Diego, CA, 1990.
(2) Baney, R. H.; Itoh, M.; Sakakibara, A.; Suzuki, T. *Chem. Rev.* **1995**, *95*, 1409−1430.
(3) Brown, J. F., Jr. *J. Am. Chem. Soc.* **1965**, *87*, 4317−4324.
(4) Feher, F. J.; Newman, D. A.; Walzer, J. F. *J. Am. Chem. Soc.* **1989**, *111*, 1741−1748.
(5) Voronkov, M. G.; Lavrentiev, V. I. *Top. Curr. Chem.* **1982**, *10*, 199−236.
(6) Agaskar, P. A.; Day, V. W.; Klemperer, W. G. *J. Am. Chem. Soc.* **1987**, *109*, 5554−5556.
(7) Eisenberg, P.; Erra-Balsells, R.; Ishikawa, Y.; Lucas, J. C.; Mauri, A. N.; Nonami, H.; Riccardi, C. C.; Williams, R. J. J. *Macromolecules* **2000**, *33*, 1940−1947.
(8) Wallace, W. E.; Guttman, C. M.; Antonucci, J. M. *Polymer* **2000**, *41*, 2219−2226.
(9) Loy, D. A.; Baugher, B. M.; Schneider, D. A. *Polym. Prepr.* **1998**, *39* (2), 418−419.
(10) Loy, D. A.; Baugher, B. M.; Baugher, C. R.; Schneider, D. A.; Rahimian, K. *Chem. Mater.* **2000**, *12*, 3624−3632.
(11) Fasce, D. P.; Williams, R. J. J.; Méchin, F.; Pascault, J. P.; Liauro, M. F.; Pétiaud, R. *Macromolecules* **1999**, *32*, 4757−4763.
(12) Lichtenhan, J.; Otonari, Y. A.; Carr, M. J. *Macromolecules* **1995**, *28*, 8435−8437.
(13) Sellinger, A.; Laine, R. M. *Macromolecules* **1996**, *29*, 2327−2330.
(14) Zhang, C.; Laine, R. M. *J. Organomet. Chem.* **1996**, *521*, 199−201.
(15) Kresge, C. T.; Leonowicz, M. E.; Roth, W. J.; Vartuli, J. C.; Beck, J. S. *Nature* **1992**, *359*, 710−712.
(16) Ukrainczyk, L.; Bellman, R. A.; Anderson, A.B. *J. Phys. Chem. B* **1997**, *101*, 531−539.
(17) (a) Inagaki, S.; Guan, S.; Fukushima, Y.; Ohsuna, T.; Terasaki, O. *J. Am. Chem. Soc.* **1999**, *121*, 961. (b) Guan, S.; Inagaki, S.; Ohsuana, T.; Terasaki, O. *J. Am. Chem. Soc.* **2000**, *122*, 5660. (c) Melde, B. J.; Holland, B. T.; Blanford, C. F.; Stein, A. *Chem. Mater.* **1999**, *11*, 3302. (d) Yoshina-Ishii, C.; Asefa, T.; Coombs, N.; MacLachlan, M. J.; Ozin, G. A. *Chem. Commun.* **1999**, *24*, 2539. (e) Asefa, T.; MacLachlan, M. J.; Coombs, N.; Ozin, G. A. *Nature* **1999**, *402*, 867. (f) Lu, F.; Fan, H.; Doke, N.; Loy, D. A.; Assink, R. A.; LaVan, D. A.; Brinker, C. J. *J. Am. Chem. Soc.* **2000**, *122*, 5258.
(18) Matějka, L.; Dukh, O.; Brus, J.; Simonsick, W. J., Jr.; Meissner, B. *J. Non-Cryst. Solids* **2000**, *270*, 34−47.
(19) Slinyakova, I. B.; Kurennaya, L. I. *Vysokomol. Soedin. Ser. B* **1972**, *14*, 889−892.
(20) Chernenko, S. P.;. Cheremukhina, G. A.; Fateev, O. V.; Smykov, L. P.; Vasiliev, S. E.; Zanevski, Yu. V.; Kheiker, D. M.; Popov, A. N. *Nucl. Instrum. Methods Phys. Res.* **1994**, *A348*, 261.
(21) Feher, F. J.; Budzichowski, T. A.; Blanski, R. L.; Weller, K. J.; Ziller, J. W. *Organometallics* **1991**, *10*, 2526−2528.
(22) Rikowski, E.; Marsmann, H. C. *Polyhedron* **1997**, *16*, 3357−3361.
(23) Stockmayer, W. H. *J. Polym. Sci.* **1952**, *9*, 69.

(24) Devreux, F.; Boilot, J. P.; Chaput, F.; Lecomte, A. *Phys. Rev.* **1990**, A *41*, 6901−6909.
(25) Ng, L. V.; Thompson, P.; Sanchez, J.; Macosko, C. W.; McCormick, A. V. *Macromolecules* **1995**, *28*, 6471−6476.
(26) Loy, D. A.; Carpenter, J. P.; Alam, T. M.; Shaltout, R.; Dorhout, P. K.; Greaves, J.; Small, J. H.; Shea, K. J. *J. Am. Chem. Soc.* **1999**, *121*, 5413−5425.
(27) Bassindale, R.; Gentle, T. E. *J. Mater. Chem.* **1993**, *3*, 1319−1325.
(28) Feher, F. J.; Budzichowski, T. A. *Organomet. Chem.* **1989**, *37*, 153−163.
(29) Rankin, S. E.; Kasehagen, L. J.; McCormick, A. V.; Macosko, C. W. *Macromolecules* **2000**, *33*, 7639−7648.
(30) Shimojima, A.; Sugahara, Y.; Kuroda, K. *Bull. Chem. Soc. Jpn.* **1997**, *70*, 2847−2853.
(31) Flory, P. J. In *Statistical Mechanics of Chain Molecules*; Interscience Publisher/J. Wiley: New York, 1969; p 42.
(32) Buckley, C. P.; Kovacs, A. J. in: *Structure of Crystalline Polymers*; Hall, I. H., Ed.; Elsevier: London, New York, 1984; Chapter 7.

MA010136X